



**HAL**  
open science

# Physical modeling of the vocal folds closure and the mucus influence

Anne Bouvet, Annemie van Hirtum, Xavier Pelorson

► **To cite this version:**

Anne Bouvet, Annemie van Hirtum, Xavier Pelorson. Physical modeling of the vocal folds closure and the mucus influence. CFM 2017 - 23ème Congrès Français de Mécanique, Aug 2017, Lille, France. hal-01582207

**HAL Id: hal-01582207**

**<https://hal.science/hal-01582207>**

Submitted on 6 Sep 2017

**HAL** is a multi-disciplinary open access archive for the deposit and dissemination of scientific research documents, whether they are published or not. The documents may come from teaching and research institutions in France or abroad, or from public or private research centers.

L'archive ouverte pluridisciplinaire **HAL**, est destinée au dépôt et à la diffusion de documents scientifiques de niveau recherche, publiés ou non, émanant des établissements d'enseignement et de recherche français ou étrangers, des laboratoires publics ou privés.

# Physical modeling of the vocal folds closure and the mucus influence

A. BOUVET<sup>a</sup>, A. VAN HIRTUM<sup>b</sup>, X. PELORSON<sup>c</sup>

*Grenoble Images Parole Signal Automatique (GIPSA-lab) - [Site web](#)*

*Université Stendhal - Grenoble III, Université Pierre-Mendès-France - Grenoble*

*II, Université Joseph Fourier - Grenoble I, CNRS : UMR5216, Institut Polytechnique de Grenoble  
- Grenoble Institute of Technology*

*GIPSA-lab, 11 rue des Mathématiques, Grenoble Campus BP46, F-38402 SAINT MARTIN  
D'HERES CEDEX - France*

a. Anne.Bouvet@gipsa-lab.grenoble-inp.fr

b. Annemie.VanHirtum@gipsa-lab.grenoble-inp.fr

c. Xavier.Pelorson@gipsa-lab.grenoble-inp.fr

## Résumé :

*Dans cette contribution, nous nous intéressons à l'étude expérimentale et à la modélisation physique de la présence de mucus à la surface des cordes vocales notamment lors de la collision des cordes vocales.*

*Afin d'étudier et de quantifier l'importance de ce phénomène, nous présentons des résultats expérimentaux obtenus sur une maquette de cordes vocales. Ce dispositif, réalisé à l'échelle 3:1, permet de simuler le mouvement des cordes vocales et de contrôler la fréquence d'oscillation et l'amplitude de déplacement. La présence de mucus est simulée en injectant de manière continue un liquide en aval de la maquette. La quantification des effets est réalisée en mesurant la pression en différentes positions le long de la maquette.*

*Les résultats expérimentaux montrant un effet important du liquide, un modèle théorique prenant en compte l'influence d'une couche de liquide sur l'écoulement est élaborée et discutée.*

## Abstract:

*In this contribution we focus on the experimental study and the physical modelling of the presence of mucus at the surface of the vocal folds, in particular during the collision of the vocal folds.*

*In order to study and to quantify this phenomenon, we first present experimental results obtained on a mechanical replica of the vocal folds. This set-up, built on 3:1 scale, allows to simulate the vocal folds motion and to control the oscillation frequency as well as the amplitude of the displacement. The presence of mucus is simulated by injecting continuously a liquid downstream from the replica. Quantification of the effects is obtained thanks to pressure sensors located along the replica.*

*Since the experimental results showed an important effect of the liquids, a theoretical model for the flow accounting for a liquid layer is derived and discussed.*

**Key words: Voice; Speech; Vocal folds; Acoustic; Flow**

# 1 Introduction

The production of voiced sounds is essentially linked to the auto-oscillation of the vocal folds. This phenomenon is the result of a fluid-structure interaction between the airflow coming from the lungs and the vocal folds' elastic tissues. The understanding and modelling of this interaction is crucial for numerous domains from speech synthesis to treatment and voice pathology prevention.

Physical modelling of the vocal folds oscillations requires a biomechanical model of the vocal folds tissues and a model of the flow through the glottis (the glottis is the space between the vocal folds). The theoretical model for the flow determines the hydrodynamic forces imposed on the tissues and is therefore essential for the modelling of the biomechanics.

In this contribution, we are interested in the mucus present on the surface of the vocal folds. The lubricating role of mucus is known to be crucial [1], but is not much studied from a physical point of view. The literature also reports that an excess, for example due to bronchial infection, or a rarefaction, due to a dehydrated environment, of the mucus affects the vocal folds vibration and hence perturbs speech production [2]. In addition, the presence of liquids can, potentially, affect the air flow, particularly during the closure of the vocal folds [3]. In this study water/air flow and oil/air flow are considered. The usage of oil is motivated since the dynamic viscosity ratio between oil and air yields 1000, which is also reported for mucus from in-vivo observations [4].

Firstly, the influence of the presence of liquids on the flow is searched experimentally. Therefore, an experimental setup is proposed in order to quantify the pressure within and upstream of a rigid glottal replica allowing to consider steady as well as unsteady geometrical conditions.

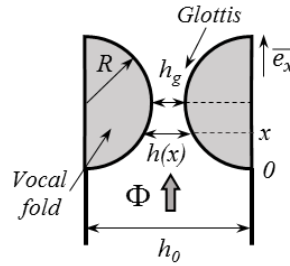


Figure 1 : Schematic representation of the glottal aperture  $h(x)$  between both vocal folds represented by a half circle with radius  $R$  in circular duct with diameter  $h_0$ .

Secondly, to analyze this phenomenon, we consider a physical model based on the classic flow model used to describe the flow in the underlying Fluid/Structure Interaction. This classical model developed in [5] describes the flow using the one dimensional, laminar, fully inviscid, steady and incompressible Bernoulli's equation to which a corrective viscous term, corresponding to a fully developed two dimensional Poiseuille flow within the glottal constriction presented in Figure 1, is added:

$$p(x) = P_0 - \frac{1}{2}\rho \frac{\Phi^2}{l_g^2} \left( \frac{1}{h(x)^2} - \frac{1}{h_0^2} \right) - 12\mu \frac{\Phi}{l_g} \int_0^x \frac{dx}{h(x)^3} \quad (1)$$

Where  $P_0$  is the upstream pressure,  $\rho$ , the fluid density at rest,  $\Phi$ , the volume flow rate,  $l_g$ , the subglottal width (transverse to the flow),  $h_0$ , the subglottal height and  $\mu$ , the dynamic viscosity coefficient of the fluid.

To take into account the multi-fluid presence (air and mucus), a two-dimensional stratified flow model is presented using the same assumptions underlying the Poiseuille term in Eq. (1). This approach is of interest since it extends the classical model approach to multi-fluids and it is an open question whether this approach remains appropriate in presence of mucus. The current work is a

first step to answer this question. The viscous model portion for stratified flow is proposed and preliminary theoretical results are presented.

## 2 Methods

### 2.1 Experimental set-up

In order to observe experimentally the effect of the liquid during phonation, an experimental set-up representing the vocal folds at a scale 3:1 and illustrated in Figure 2 and Figure 3 has been developed.

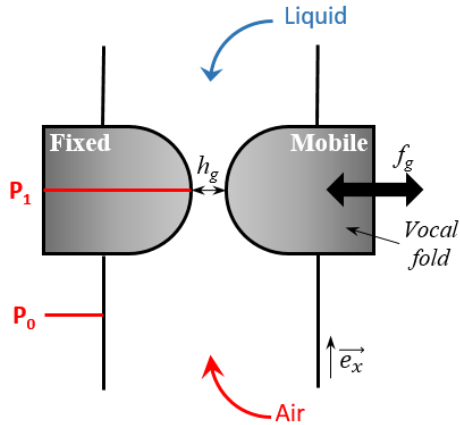


Figure 2: Global drawing of the experimental vocal folds set-up

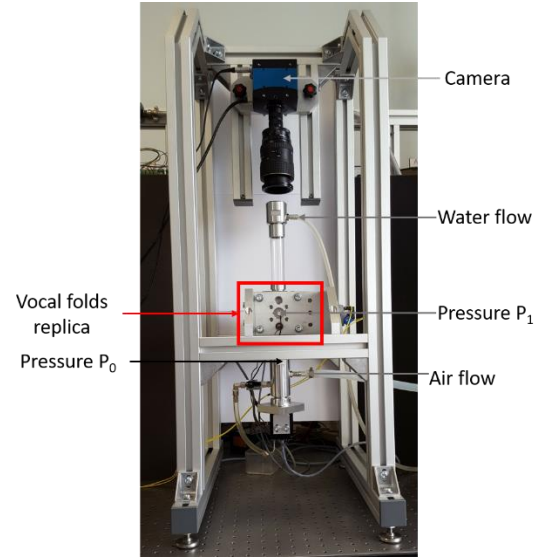


Figure 3: Picture of the experimental rigid vocal folds set-up

An air facility (Atlas Copco, GA5 FF-300-8), equipped with pressure regulator (Norgren, 11-818-987) and a manual valve is used to supply airflow through a mechanical replica of the trachea, larynx and vocal tract.

The rigid vocal fold replica consists of two rigid half cylinders (radius  $R=1$  cm, width  $l_g=2.5$  cm) placed in a uniform circular duct of diameter 2.5 cm. The duct downstream from the replica (length 12.5 cm) and upstream from the replica (length 20 cm) represent the vocal tract and trachea, respectively. It is noted that the resulting glottal aperture has a rectangular shape corresponding to the aspect ratio  $l_g/h_g$  observed on human speakers during normal vocal folds auto-oscillation [6].

Consequently, the glottal area in the streamwise direction is given as  $A(x) = h(x) \times l_g$  where the minimum area is given as  $A_g = h_g \times l_g$ .

In order to generate time-varying geometrical conditions, the glottal aperture,  $h_g$  can be varied in a controlled way using a forced movement of one vocal fold replica imposed by a step-motor. A quasi-sinusoidal movement is imposed with a frequency up to 10 Hz while the amplitude of the motion varies in the range of 0 mm up to 1.4 mm. 0 mm indicates glottal closure.

Liquid is supplied at a distance of 10.5 cm downstream from the glottal replica along the walls of the vocal tract replica, as depicted in Figure 2. In this study, distilled water (density:  $\rho = 1000 \text{ kg.m}^{-3}$ , viscosity:  $\mu = 1.002 \times 10^{-3} \text{ Pa.s}$ ) or mineral oil (density:  $\rho = 850 \text{ kg.m}^{-3}$ , viscosity:  $\mu = 212.5 \times 10^{-3} \text{ Pa.s}$ ) were used.

Pressure transducers (Kulite XCS-093) are placed in the flow channel as shown in Figure 2 in order

to measure  $P_0$  and  $P_1$ , respectively the subglottal pressure and the pressure at the minimum constriction height  $h_g$ . This quantity is of importance as it measures the forces generated by the flow on the vocal folds. The pressure transducers were calibrated against a watermeter with a precision of  $\pm 2.5$  Pa.

The minimum height,  $h_g$  is measured by means of an optical sensor (type OPB700) with  $10^{-2}$  mm estimated uncertainty in the measurement.

Time-varying signals of pressure ( $P_0(t)$  and  $P_1(t)$ ) and minimum constriction height ( $h_g(t)$ ) are gathered with a sample frequency of 10000 Hz, using a data-acquisition system (National Instruments, PCI-MIO-16XE-10) controlled with LabView [1].

Finally, the oscillation of the replica is recorded using a high-speed camera (Motion BLITZ Eosens Cube 7) at a 525 frames per second with an aperture time of 750  $\mu$ s. The position of the camera is pictured in Figure 3.

## 2.2 Theoretical stratified flow model

A stratified flow model is presented to take in account up to three layers of immiscible fluids. In addition, the channel inclination is accounted for. This way, compared to equation (1), a term is added for channel's inclination and the viscous term on the right hand side is studied to take into account different fluid layers. The  $90^\circ$  inclination corresponds to the experimental configuration presented in Section 2.1. A two-dimensional (2D) uniform channel of height  $H$  is filled with up to three fluids, typically liquid/gas/liquid, as shown in Figure 4.

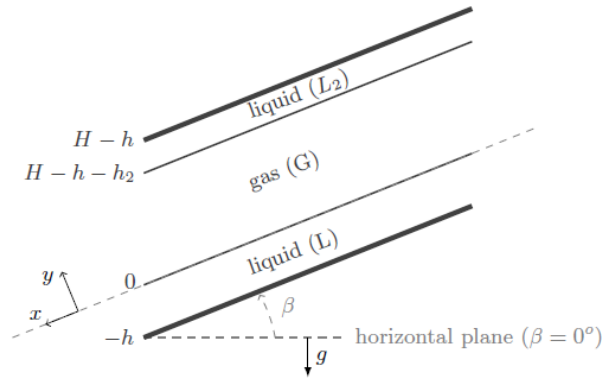


Figure 4: Schematic overview of the stratified flow configuration:  $x$ -direction parallel to rigid channel walls, orthogonal  $y$ -axis, channel inclination angle  $0 \leq \beta \leq 90^\circ$ , total channel height  $H$ .

Gas (G) layer enveloped by two liquid layers (L,  $L_2$ ) of height  $h$  and  $h_2$  respectively. The  $y$ -coordinates associated with outer channel walls ( $y = -h$  and  $y = H - h$ ) and smooth fluid interfaces ( $y = 0$  and  $y = H - h - h_2$ ) are indicated as is gravitational acceleration  $g$ .

Steady pressure driven laminar fully developed stratified flow is considered for one up to three layers of immiscible fluids (subindex  $i = \{L, G, L_2\}$ ) subjected to gravity. The layer thicknesses and axes are taken as depicted in Figure 1. Interfaces between fluids are assumed smooth with dynamic viscosity  $\mu_i$  and density  $\rho_i$ . Under these assumptions the momentum equation associated with the flow in each layer yields the following set of second order partial differential equations where  $u_L$ ,  $u_G$  and  $u_{L_2}$  indicate the velocity profile in each layer respectively,  $\beta$  denotes the inclination angle and  $\frac{dp}{dx}$  denotes the driving pressure gradient:

$$\mu_L \frac{\partial^2 u_L}{\partial y^2} = \frac{dp}{dx} - \rho_L g \sin(\beta);$$

$$-h \leq y < 0,$$

$$\mu_G \frac{\partial^2 u_G}{\partial y^2} = \frac{dp}{dx} - \rho_G g \sin(\beta);$$

$$0 \leq y \leq H - h - h_2,$$

$$\mu_{L_2} \frac{\partial^2 u_{L_2}}{\partial y^2} = \frac{dp}{dx} - \rho_{L_2} g \sin(\beta);$$

$$H - h - h_2 < y \leq H - h.$$

No-slip wall boundary conditions are applied at lower ( $y = -h$ ) and upper ( $y = H - h$ ) interior wall

$$u_L|_{y=-h} = 0,$$

$$u_{L_2}|_{y=H-h} = 0,$$

and interface conditions express equal velocity and shear along the lower ( $y = 0$ ) and upper ( $y = H - h - h_2$ ) liquid/gas interface:

$$u_L|_{y=0} = u_G|_{y=0}, \quad u_G|_{y=H-h-h_2} = u_{L_2}|_{y=H-h-h_2},$$

$$\mu_L \frac{\partial u_L}{\partial y} \Big|_{y=0} = \mu_G \frac{\partial u_G}{\partial y} \Big|_{y=0}, \quad \mu_G \frac{\partial u_G}{\partial y} \Big|_{y=H-h-h_2} = \mu_{L_2} \frac{\partial u_{L_2}}{\partial y} \Big|_{y=H-h-h_2}.$$

Analytical expressions for the fully developed laminar velocity profiles ( $u_L$ ,  $u_G$ ,  $u_{L_2}$ ) in each layer are then obtained by integrating momentum Eq. (1). Expressions simplify further when assuming that outer layers contain the same fluid (identical  $\rho$  and  $\mu$ ). Consequently, mean velocities within each layer are obtained and all quantities of interest can be deduced and expressed as a function of mean velocity, Reynolds number or driving pressure. It has been verified that in the case of a single fluid ( $H=h=h_2$ ) expressions reduce to well-known Poiseuille flow used in Eq. (1).

## 3 Results

### 3.1 Experimental results

In the following, experimental results corresponding to two different situations will be presented: oscillation without (Section 3.1.1) and with (Section 3.1.2) complete closure.

#### 3.1.1 Oscillation without complete closure

In a first series of experiments, the vocal folds replica oscillates without a complete closure. The amplitude of the forced motion varied between [0.75 1.9] mm. An example of results, obtained using the injection of mineral oil, is presented in Figure 5 and compared to the situation when no liquid is present (dry configuration).

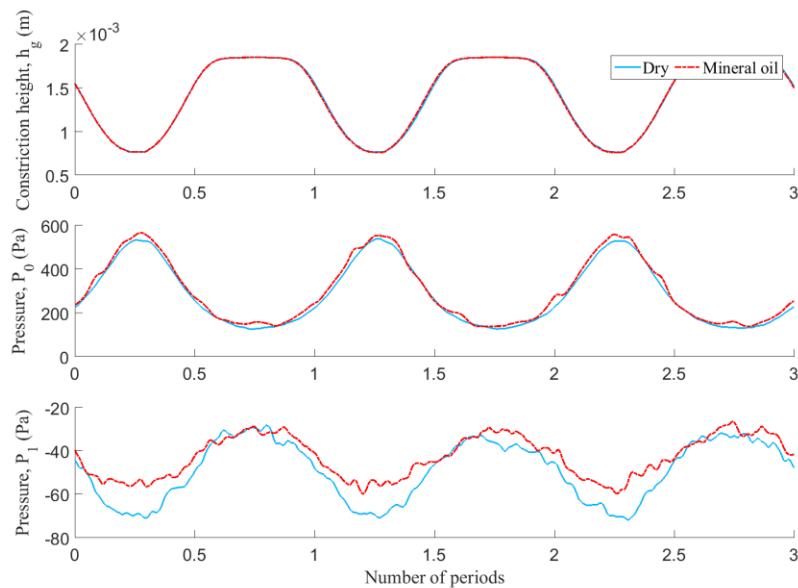


Figure 5: Experimental results of aperture height (0.75-1.9 mm) and pressure without and with mineral oil (Vaseline oil), for an imposed movement of 9 Hz.

As can be seen in Figure 5, the injection of mineral oil reduces the glottal pressure,  $P_1$  by 13% and thus the hydrodynamic forces on the vocal folds. More precisely, one can observe that the major effect occurs during the closure and opening phase of the replica where a reduction of 27 % has been measured.

### 3.1.2 Oscillation with complete closure

In this second set of experiments, measurements have been realized in a condition where the vocal folds closed completely. The amplitude of the forced motion varied between [0 1.4] mm. An example of results, corresponding to the injection of distilled water, is presented in Figure 6 and compared to the situation when no liquid is present (dry configuration).

Two configurations are considered Figure 6. The configuration “Water 1” corresponds to the initial injection of distilled water at a  $12 \text{ ml.s}^{-1}$  rate. The configuration “Water 2” corresponds to a later situation where a saturation of liquid is obtained. This would correspond to a pathological situation.

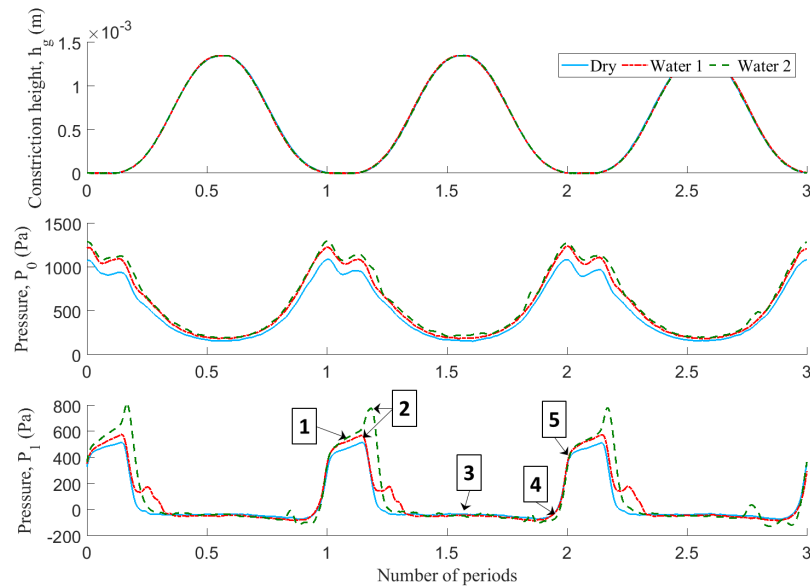


Figure 6: Experimental results of aperture height (0-1.4 mm) and pressure without distilled water, then with two configurations with liquid presence for an imposed movement of 9 Hz. Number [1-5] correspond to images shown in Figure 7.

In both configurations, the presence of a liquid is mainly visible during the opening of the vocal folds replica. Compared with the dry configuration, the liquid has a direct influence on the pressure,  $P_1$  with an increase of 60 Pa and 290 Pa depending on the configuration.

This effect is likely due to the liquid preventing the opening of the glottis. As a result the closure increases up to 10% of a cycle period in configuration “Water 1” and 3.5% in configuration “Water 2”.

In Figure 7, pictures obtained from the high speed video recordings illustrate this phenomenon during a single oscillation cycle. Corresponding pressure measurements are indicated in Figure 6.



Figure 7: Imaging of an oscillation cycle of the rigid vocal folds with distilled water presence.

### 3.2 Stratified flow model results

As for the experiments, the stratified 2D viscous flow model is assessed for water/air flow and oil/air flow. The dynamic viscosity ratio between these fluids yields 50 and 1000, respectively. The density ratio yields 1000 and 860, respectively.

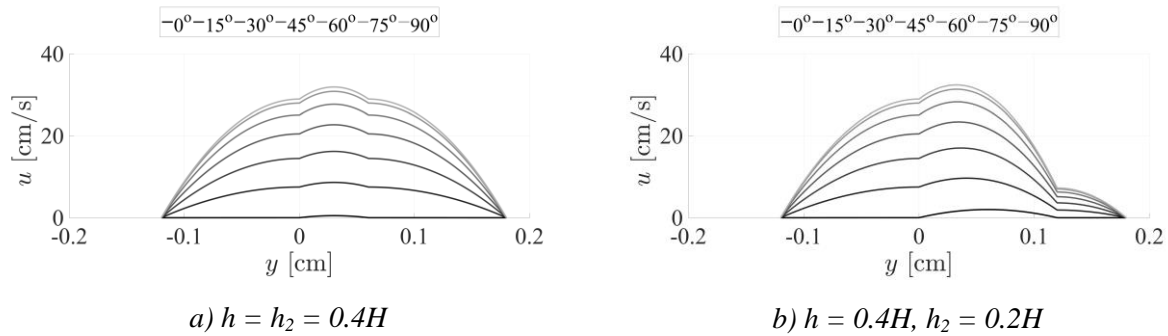


Figure 8 : Stratified flow velocity profiles for  $H = 0.3$  cm and  $dp/dx = -0.2$  for different inclination angles  $\beta$ : a) symmetry oil/air and b) asymmetry oil/air. Lines shift from dark to light gray as  $\beta$  increases.

Examples of velocity profiles showing the influence of inclination angle  $\beta$  and flow configuration are presented in Figure 8 for oil/air in the case of layer thickness symmetry and asymmetry for a channel with constant height  $H=0.3$  cm and driving pressure difference  $-0.2$ . The influence of the ratio  $h/H$  on the overall maximum velocity and its associated  $y$ -position is further illustrated in Figure 9. A different tendency is observed for thin and thick liquid layers for both the maximum value as its position. When majority of the channel is occupied by gas the maximum velocity decreases slightly (less than 50%), however when liquid becomes predominant, the maximum value increases until it is multiplied by almost a factor four for a vertical channel ( $90^\circ$ ). Further increasing the liquid layer thickness reduces the maximum velocity strongly (factor more than 100). For this asymmetrical configuration, for thin liquid layers it is seen that the position of the maximum velocity gradually shifts from the horizontal case (slope 1/2) to the slope for an inclined channel (slope 1) in the case of thick liquid layers until liquid fills the channel and maximum velocity occurs at the center of the channel as expected for single phase flow. The rate of change from one slope to the other depends on the inclination angle.

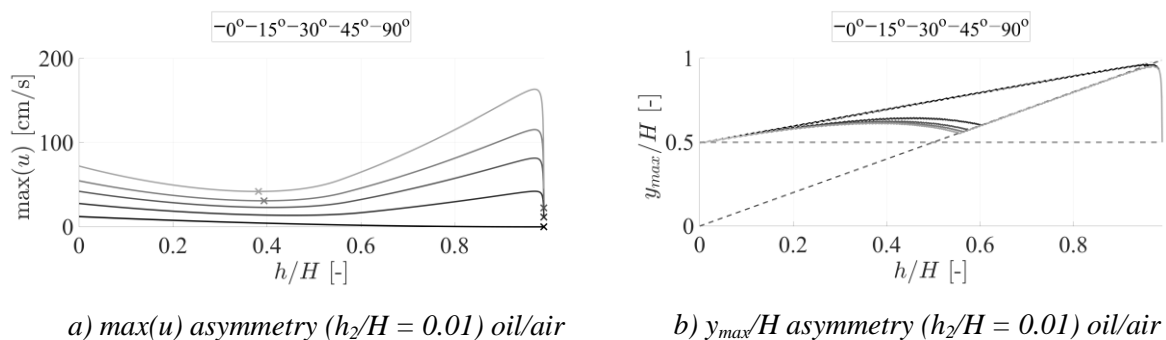


Figure 9: Maximum velocity  $\max(u)$  and its normalized position  $y_{\max}/H$  for  $H = 0.3$  cm and  $dp/dx = -0.2$  as a function of normalized liquid layer thickness  $h/H$  for different inclination angles  $\beta$ . Lines shift from dark to light gray as  $\beta$  increases.

Maximum velocity normalized by the overall mean velocity  $\max(u)/\bar{u}$  as a function of  $h/H$  for different configurations of the upper liquid layer in the case of a vertical channel is further illustrated in Figure 10. The change in tendency as a function of liquid layer thickness is again observed. Moreover, the ratio is seen to deflect from  $3/2$ , the constant value in the case of single phase flow, to a degree depending on the flow configuration indicating that the flow is locally

accelerated or decelerated compared to single phase flow. Figure 11 illustrates variation of normalized pressure difference  $\Delta P_N$  (top) and mean velocity in the gas layer (middle) when a constant mean velocity is imposed in the liquid layer and the channel height  $H$  is varied sinusoidal (bottom) for constant liquid layer thicknesses. The pressure difference is normalized by the pressure difference for dispersed flow. When the channel is fully filled with liquid normalization is done with respect to pure liquid flow so that the resulting pressure ratio yields 1 for the minimum assessed channel height. Both quantities vary to a factor 2 or more.

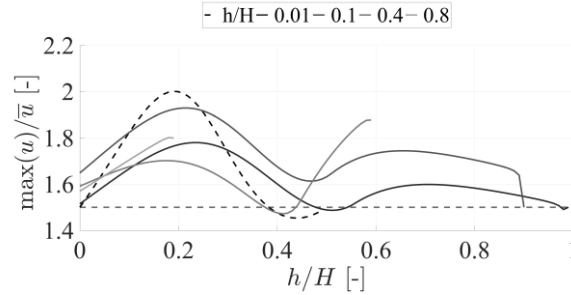


Figure 10 : Ratio of maximum to mean velocity  $\max(u)/\bar{u}$  for oil/air,  $H = 0.3$  cm and  $dp/dx = -0.2$  as a function of normalized liquid layer thickness  $h/H$  for vertical channel ( $\beta=90^\circ$ )  $\max(u)/\bar{u} = 3/2$  is indicated (horizontal dashed line). Liquid layer thickness symmetry ( $h_2=H = h=H$ , dark dashed curve) and asymmetry (constant  $h_2=H$ , full lines)

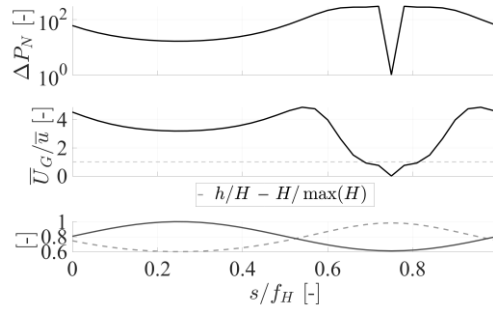


Figure 11: Illustration of  $\Delta P_N$  (top), driving pressure for oil/air stratified flow normalized with respect to single phase dispersed flow and  $\bar{U}_G/\bar{u}$  (middle), mean velocity in the gas layer normalized by overall mean velocity for  $\bar{U}_L=200$  cm/s and varying channel height  $h+h_2 \leq H \leq \max(H)$  (full line, bottom) with  $\max(H)=0.3$  cm and  $h_2/\max(H)=0.01$  held constant for a vertical ( $\beta = 90^\circ$ ) channel: liquid layer asymmetry  $h/\max(H)=0.6$ . The ratio  $h/\max(H)$  (dashed line, bottom) and  $\bar{U}_G/\bar{u}=1$  (dashed line, middle) are plotted as a reference.

## 4 Conclusion

This contribution presents the first steps in a long term study of the influence of mucus and liquids at the surface of the vocal folds during phonation. Experimental results confirmed that the presence of liquids significantly affect the air flow through the glottis. When collision of the folds is allowed, this phenomenon is mainly visible during the closure and opening of the vocal folds. Since, perceptually, the most important higher harmonics are generated during this period of time, it is expected that the effect of liquids can be of major importance.

From the presented stratified flow model it is seen that main quantities vary from a small

factor ( $< 2$ ) up to a large factor ( $>100$ ) depending on the flow configuration. This illustrates the importance of accurate quantification of the flow configuration when aiming to apply the flow model for practical purposes.

Follow-up studies will be carried on in order to test different liquids, to vary the density and the viscosity and approach the mucus properties. Also tests will be done on a second experimental set up of self-oscillating deformable vocal folds replica [7].

## Acknowledgement

This work was partly supported by the Art Speech project (ANR-15-CE23-0024)

## References

- [1] S. Ayache, M. Ouaknine, P. Dejonkere, P. Prindere and A. Giovanni. Experimental Study of the effects of Surface Mucus Viscosity on the Glottic Cycle. *J. Voice*, 18(1):107-15, 2004.
- [2] K. Verdolini-Marston, I. Titze, and D. Druker. Changes in phonation threshold pressure with induced conditions of hydration. *J. Voice* 4:142-151, 1990.
- [3] M. Döllinger, F. Gröhn, D. A. Berry, U. Eysholdt, and G. Luegmair. Preliminary Results on the Influence of Engineered Artificial Mucus Layer on Phonation. *Journal of Speech, Language, and Hearing Research*, 57:637–647, 2014.
- [4] S. K. Lai, Y.-Y. Wang, D. Wirtz, and J. Hanes. Micro- and macrorheology of mucus. *Adv. Drug Deliv. Rev.* 61(2):86-100, 2009.
- [5] J. Cisonni, A. Van Hirtum, X. Pelorson, and J. Willems. Theoretical simulation and experimental validation of inverse quasi one-dimensional steady and unsteady glottal flow models. *J. Acoust. Soc. Am.*, 124(1):535–545, 2008.
- [6] J. G. Švec, On vibration properties of human vocal fold. PhD Rijksuniversiteit Groningen, The Netherlands. 2000.
- [7] J. Haas, P. Luizard, X. Pelorson, and J.C. Lucero. Study of the effect of a moderate asymmetry on a replica of the vocal folds. *Acta Acustica*, 102:230–239, 2016.